

# Optical and Visual Quality With Physical and Visually Simulated Presbyopic Multifocal Contact Lenses

Maria Vinas<sup>1</sup>, Sara Aissati<sup>1</sup>, Ana Maria Gonzalez-Ramos<sup>1</sup>, Mercedes Romero<sup>1</sup>, Lucie Sawides<sup>2</sup>, Vyas Akondi<sup>1,3</sup>, Enrique Gamba<sup>2</sup>, Carlos Dorransoro<sup>1,2</sup>, Thomas Karkkainen<sup>4</sup>, Derek Nankivil<sup>4</sup>, and Susana Marcos<sup>1</sup>

<sup>1</sup> Instituto de Optica, Consejo Superior de Investigaciones Cientificas (IO-CSIC), Madrid, Spain

<sup>2</sup> EyesVision, Madrid, Spain

<sup>3</sup> Byers Eye Institute, Stanford University, Palo Alto, CA, USA

<sup>4</sup> Johnson & Johnson Vision, Inc., Research & Development, Jacksonville, FL, USA

**Correspondence:** Maria Vinas, Instituto de Optica, Consejo Superior de Investigaciones Cientificas (CSIC), Madrid, Spain, C/Serrano, 121, Madrid, 28006, Spain. e-mail: [maria.vinas@io.cfmac.csic.es](mailto:maria.vinas@io.cfmac.csic.es)

**Received:** June 30, 2020

**Accepted:** August 24, 2020

**Published:** September 22, 2020

**Keywords:** multifocal contact lenses; presbyopia; visual simulators

**Citation:** Vinas M, Aissati S, Gonzalez-Ramos AM, Romero M, Sawides L, Akondi V, Gamba E, Dorransoro C, Karkkainen T, Nankivil D, Marcos S. Optical and visual quality with physical and visually simulated presbyopic multifocal contact lenses. *Trans Vis Sci Tech.* 2020;9(10):20, <https://doi.org/10.1167/tvst.9.10.20>

**Purpose:** As multifocal contact lenses (MCLs) expand as a solution for presbyopia correction, a better understanding of their optical and visual performance becomes essential. Also, providing subjects with the experience of multifocal vision before contact lens fitting becomes critical, both to systematically test different multifocal designs and to optimize selection in the clinic. In this study, we evaluated the ability of a simultaneous vision visual simulator (SimVis) to represent MCLs.

**Methods:** Through focus (TF) optical and visual quality with a center-near aspheric MCL (low, medium and high near adds) were measured using a multichannel polychromatic Adaptive Optics visual simulator equipped with double-pass, SimVis (temporal multiplexing), and psychophysical channels to allow measurements on-bench and in vivo. On bench TF optical quality of SimVis-simulated MCLs was obtained from double-pass (DP) images and images of an E-stimulus using artificial eyes. Ten presbyopic subjects were fitted with the MCL. Visual acuity (VA) and DP retinal images were measured TF in a 4.00 D range with the MCL on eye, and through SimVis simulations of the same MCLs on the same subjects.

**Results:** TF optical (on bench and in vivo) and visual (in vivo) quality measurements captured the expected broadening of the curves with increasing add. Root mean square difference between real and SimVis-simulated lens was 0.031/0.025 (low add), 0.025/0.015 (medium add), 0.019/0.011 (high add), for TF DP and TF LogMAR VA, respectively. A shape similarity metric shows high statistical values (lag  $\kappa = 0$ ),  $\rho = 0.811/0.895$  (low add),  $0.792/0.944$  (medium add), and  $0.861/0.915$  (high add) for TF DP/LogMAR VA, respectively.

**Conclusions:** MCLs theoretically and effectively expand the depth of focus. A novel simulator, SimVis, captured the through-focus optical and visual performance of the MCL in most of the subjects. Visual simulators allow subjects to experience vision with multifocal lenses prior to testing them on-eye.

**Translational Relevance:** Simultaneous visual simulators allow subjects to experience multifocal vision non-invasively. We demonstrated equivalency between real multifocal contact lenses and SimVis-simulated lenses. The results suggest that SimVis is a suitable technique to aid selection of presbyopic corrections in the contactology practice.

## Introduction

Multifocal contact lenses (MCLs) are increasingly used to correct presbyopia, the age-related loss of the accommodative amplitude in the eye.<sup>1-4</sup> However, understanding of the optical and perceptual impact of MCLs at the individual level is needed to identify the visual compromise of the various lens designs and select the optimal lens for a patient.

MCLs rely on the principle of simultaneous vision, where image quality of an image at far is slightly reduced to gain vision at near. There are multiple MCL designs (mostly refractive, and rotationally symmetric),<sup>2-4</sup> with differences primarily in radial variation in refractive power (from abrupt changes between near and far zones to aspheric extended-depth-of-focus designs), on the region of the pupil devoted for near and far (center-near or center-distance vision), or the number of alternating zones for near and far (i.e., from two to five alternating zones).<sup>4</sup> Some manufacturers offer MCLs with slight variations of the design according to age, to account for age-dependent changes in pupil diameter, and to refractive error.<sup>5</sup>

Despite the increasing number of MCLs,<sup>6,7</sup> prediction of their success prior to being prescribed in subjects is complicated. Several reports evaluate MCLs on eye in terms of through-focus (TF) visual acuity (VA) or contrast sensitivity measurements, in some cases in comparison with monovision (one eye corrected for far, the other one for near).<sup>8-11</sup> Generally, to understand intersubject variability of lens performance, researchers evaluate the impact of certain factors including pupil diameter or ocular aberrations.<sup>12-14</sup> However, this type of evaluation is time- and resource-consuming and only allows a posteriori evaluation of visual performance. Besides, many clinical evaluations rely on patient satisfaction questionnaires. However, from those subjective evaluations it is sometimes difficult to disentangle dissatisfaction originating from the optical design and its perceptual tolerance from those associated to lens wear comfort.<sup>2</sup>

Adaptive optics (AO) visual simulators are particularly attractive to test vision in subjects with new optical designs before delivering or even manufacturing a lens.<sup>15-19</sup> AO-simulations of new corrections enable investigation of interactions between a subject's optics and a given correction, characterization of differences across corrections, and eventually selection of the correction that optimizes perceived visual quality and performance in subjects.<sup>20</sup> In previous studies,<sup>15,16</sup> we have simulated diverse novel refractive multifocal designs (concentric and asymmetric), as well as commercial refractive and diffractive Intraoc-

ular lenses (IOLs) using a spatial light modulator (SLM) integrated in an AO system, and demonstrated equivalency between the patient's vision through the simulated lenses and physical lathe-manufactured phase-plates or physical IOLs in a cuvette.

Simultaneous vision simulators are specifically suited to simulate multifocal corrections, allowing systematic evaluation of multifocal designs. A two-channel visual simulator has been used to evaluate the effect of the magnitude of the near addition in visual degradation for far,<sup>21</sup> the pupillary distribution of far and near zones in a bifocal design,<sup>22</sup> or the orientation of asymmetric bifocal corrections.<sup>18</sup> A simultaneous vision technology has been recently developed<sup>23,24</sup> based on the concept of temporal multiplexing of an optotunable lens driven at a speed above the temporal integration of the visual system (Sim+Vis Technology, or SimVis). The through-focus performance of a given multifocal pattern is mapped into a temporal pattern defining the time that the optotunable lens spends at a given optical power, corrected by the dynamic effects of the tunable lens.<sup>25</sup> Advantages of the SimVis over standard AO-based visual simulators include the fact that it is see-through, it provides a large field of view (20°), and it is very compact. These features have allowed for the concept to be translated into a binocular, wearable clinical device (SimVis Gekko). Previous studies have proven the capability of the SimVis technology to replicate vision with real refractive segmented IOLs and trifocal diffractive IOLs<sup>20</sup> and a high correspondence between preoperative vision with SimVis Gekko and postoperative vision with the real implanted multifocal IOL.<sup>26</sup>

The ability of SimVis technology to allow subjects to noninvasively experience multifocal vision is highly useful before intraocular lens implantation, given that a lack of tolerance to implanted multifocal IOLs may require surgical explantation.<sup>27</sup> It is also useful for the patient and clinician to be able to compare across different multifocal options as a tool to guide decision. Likewise, SimVis can allow the prospective multifocal contact lens wearers to test vision with different MCL designs before putting them on their eyes. It is conceivable to use this technology to go through an MCL fitting protocol using MCLs programmed in the SimVis Gekko, largely reducing chair time, the number of physical lenses used, and patient's discomfort.

In this study, we programmed, for the first time, MCL profiles using the SimVis technology in an AO visual simulator, and tested real and simulated MCLs (center-near aspheric CLs) in subjects. We compared visual quality through focus with the real and simulated MCLs, and validated the accuracy of SimVis to replicate visual performance with those lenses.

## Methods

Through-focus optical and visual quality with real MCLs on-eye and SimVis simulations of the same MCLs on the same subjects were evaluated using a multichannel polychromatic Adaptive Optics visual simulator equipped with a double-pass channel, a SimVis channel, and a psychophysical channel to allow measurements on-bench and in vivo.

### Multifocal Contact Lenses

The MCLs used in the study were the center-near aspheric 1-Day Acuvue Moist Multifocal (Johnson & Johnson Vision Care, Jacksonville, FL, USA; Etafilcon A with LACREON technology, 58% water content). In this type of simultaneous vision solutions,<sup>12</sup> light rays passing through the pupil to form the retinal image encounter a smooth transition in power between distance and near corrections. Thus any region of the retina receives both in-focus and out-of-focus images. Aspheric lens designs have a gradual change of curvature along one of their surfaces (anterior or posterior) based on the geometry of conic sections. In center-near aspheric lenses, the higher power is in the central part and decreases progressively toward the periphery.

In the 1-Day Acuvue Moist Multifocal, the design is a hybrid back curve design (BC 8.4; Diam 14.3 mm), with a gradual change in power between near and distance zones.<sup>28</sup> There is no distinct relative plus power to the distance prescription in the low add power lens. This lens shows no distinct transition point between the near and distance powers within the optical zone. The spherical periphery aims at helping centration of the optics over the pupil. There are 61 distance powers (in 0.25 D steps from +6.00D to -9.00D) with three different add powers: low, +1.25 D; medium, +1.75 D; high, +2.50 D.

### AO Visual Simulator

Measurements were performed in a custom-developed polychromatic AO system at the Visual Optics and Biophotonics Lab (Institute of Optics, Spanish National Research Council, IO-CSIC, Madrid, Spain), described in detail in previous publications.<sup>26,29</sup> For the purposes of this study, the visual stimulus was seen through two different active optical elements: (1) a reflective deformable mirror (DM), used in this study to correct the aberrations of the optical system; and (2) a simultaneous vision simulator (Sim+Vis Technology), based on temporal

multiplexing of an optotunable lens, used to simulate the MCL design.

The current configuration of the system is formed by eight different channels, the following of which were used in this study:

- (1) The illumination channel, with light coming from the Supercontinuum laser source (SCLS, SC400 femtopower 1060 supercontinuum laser; Fianium Ltd, Southampton, UK) in combination with a dual acousto-optic tunable filter (AOTF) module (Gooch & Housego, Ilminster, UK), which delivers light in multiple wavelengths through two different fiber outputs (visible [VIS] and near infrared [NIR]). Illumination coming from the VIS channel is also used to monochromatically illuminate the visual stimuli. In this study, a visible wavelength (555 nm) was used to illuminate the visual display and to collect TF double pass (DP) retinal images (on bench and in subjects) and one-pass (1P) images (on bench). Aberrations of the system were corrected at 827 nm.
- (2) The AO channel, consisting of the Hartmann-Shack wavefront sensor (microlens array  $40 \times 32$ , 3.6 mm effective diameter, centered at 1062 nm; HASO 32 OEM; Imagine Eyes, Orsay, France) and the electromagnetic deformable mirror (DM) (52 actuators, 15-mm effective diameter, 50- $\mu\text{m}$  stroke; MIRA0, Imagine Eyes, France) to measure and correct the high order aberrations (HOAs), respectively. In this study it was used to compensate for the system aberrations and to measure the subjects' aberrations.
- (3) The SimVis channel, placed in a conjugate pupil plane of the system, consists of an optotunable lens (EL-10-30-C; Optotune Inc., Zurich, Switzerland). The DM, the wavefront sensor, and the SimVis are conjugate to the pupil by different relay lenses. Magnification from the pupil is  $2\times$  to the DM,  $1\times$  to the SimVis plane, and  $0.5\times$  to the wavefront sensor.
- (4) The retinal imaging channel captures retinal images of a 250- $\mu\text{m}$  point source and consists of a CCD camera (Retiga 1300, CCD Digital Camera, 12-bit, Monochrome,  $6.7 \times 6.7 \mu\text{m}$  pixel size,  $1024 \times 1280$  pixels; QImaging, Surrey, Canada), and a collimating lens, used for the double-pass retinal imaging (2P) channel. The laser beam is filtered before entering the eye by means of a spatial filter composed of a microscope objective ( $20\times$ ), a 25  $\mu\text{m}$ -pinhole and a 100-mm lens. This channel acts in fact as a "one-and-a-half pass," with the aerial image being the autocorrelation<sup>30</sup>

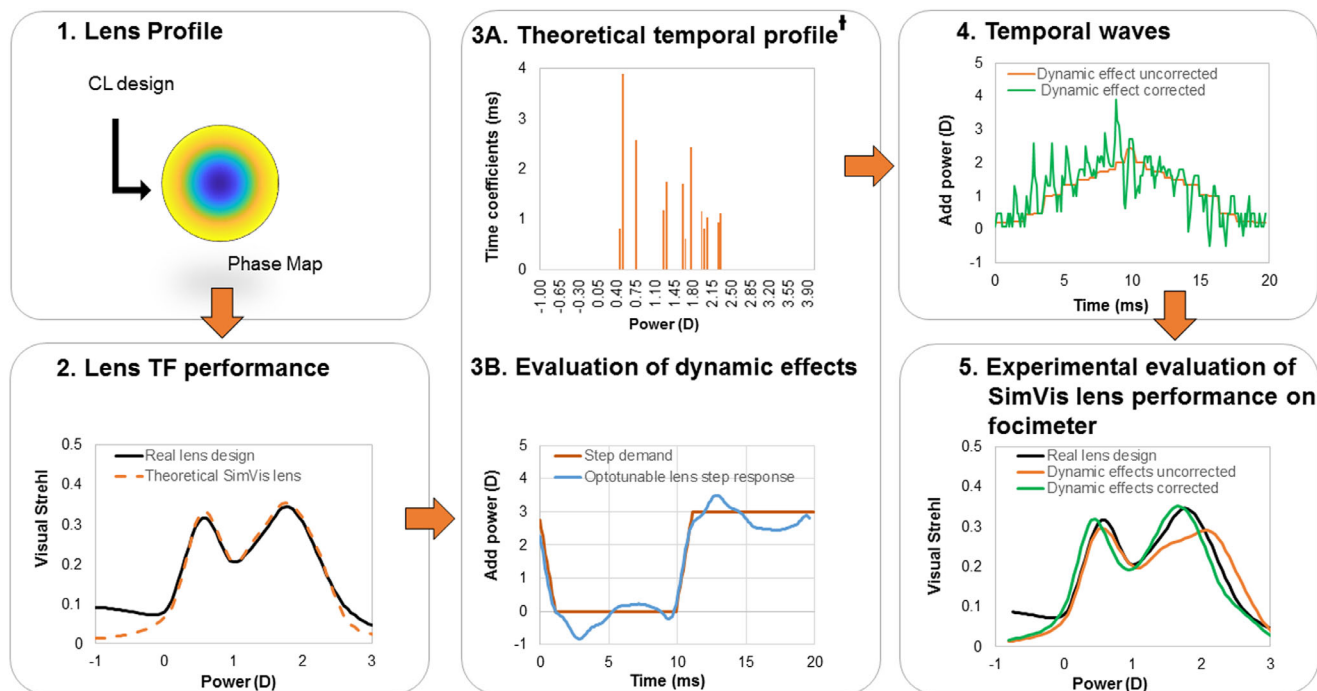


**Figure 1.** SimVis programmed lens characterization and validation of a lens design. (1) Calculation of the wave aberration (phase map) from the power map of the lens design. (2) Calculation of the through focus performance (Visual Strehl optical metric). (3A) Theoretical temporal profile.<sup>24</sup> (3B) Estimation of the SimVis temporal coefficients obtained through an iterative optimization procedure.<sup>31</sup> (4) Experimentally evaluated dynamic response of the tunable lens: its impulse response function is used to calculate the temporal corrected wave. (5) Through-Focus performance of the real lens (theoretical) and the SimVis programmed lens, with and without the correction of dynamic effects, measured using a high-speed dynamic focimeter<sup>25</sup> provided with a high-speed camera (3823 fps).

of the image of the laser spot with a 2-mm entry beam and that with a 1-mm exit beam.

- (5) The psychophysical channel uses a digital micro-mirror device (DMD) (DLP Discovery 4100 0.7 XGA; Texas Instruments, Dallas, TX, USA), placed in a conjugate retinal plane, to display visual stimuli subtending 1.62 angular degrees. The DMD was monochromatically (555 nm) illuminated with light coming from the SCLS.
- (6) The pupil monitoring channel consists of an IR camera, in combination with an IR ring of LEDs, conjugated to the eye's pupil.
- (7) The Badal optometer channel corrects for defocus in AO, SimVis- and psychophysical-channels and allows for TF psychophysical testing.

All optoelectronic elements of the system (SCLS main source, Badal system, retinal and pupil cameras, Hartmann-Shack wavefront sensor, deformable mirror and SimVis) are automatically controlled and synchronized using custom-built software programmed in Visual C++ and C# (Microsoft, Redmond, WA, USA) and Matlab (MathWorks, Natick, MA, USA). Subjects were stabilized using a dental impression and are

aligned to the system (using an x-y-z stage moving a bite bar) with the line of sight as a reference while the natural pupil is viewed on the monitor. To ensure selected pupil diameter during the measurements, a 4-mm artificial pupil was placed in a conjugate pupil plane.

## SimVis Simulations

The SimVis temporal profiles for each MCL (low, medium and high add powers) were estimated from calculations of the corresponding TF optical quality. All calculations were performed for a  $-5.00$  D refractive power lens and 4-mm pupil diameters. Computer simulation showed that in these conditions, the differences in the TF optical quality produced by design differences across lens power were negligible (root mean square [RMS] difference  $< 0.004$ , between the curves corresponding to  $+2.50$  and  $-5.50$  D, the most extreme powers in our sample). Figure 1 illustrates (for the high-add MCL design and 4-mm pupil diameter) the five steps of validation of a SimVis programmed lens.

First, the wave aberration map (Phase Map) of each lens was calculated from the corresponding power



maps provided by the manufacturer (Fig. 1.1). Then, the MTF was estimated from the wave aberration and pupil function using Fourier optics. The Visual Strehl ratio (VS) was used as an optical quality metric, estimated as the neural contrast sensitivity weighted modulation transfer function (MTF) of the system.<sup>31,32</sup> The through-focus lens performance was thus evaluated (Fig. 1.2). The calculation of the series of SimVis temporal coefficients describing a lens from the theoretical TF calculation has been described before<sup>23–25</sup> and is based on the equation described by Akondi et al.,<sup>24</sup>

$${}^+q = k \sum_{i=1}^n (t_i) (Q_i)$$

where  ${}^+q$  is the multifocal real lens pattern,  $t_i$  are the temporal coefficients (least squares with nonnegativity constraints), and  $Q_i$  is the monofocal term, in a certain through focus range (−1.00 to +3.00 D in steps of 0.05 D). These temporal coefficients stand for the weighting factors of a series of defocused monofocal PSFs, tuned to match the TF optical quality of the MCL design in an iterative optimization procedure to obtain the theoretical temporal profile of the lens (Fig. 1.3A).

In parallel we evaluated the dynamic behavior of the optotunable lens that will be used to simulate the MCL designs (Fig. 1.3B). Its impulse response function<sup>33</sup> was used, along with the theoretical temporal profile of the lens, to calculate the temporal “corrected wave” in an iterative optimization of the electrical input signal driving the lens where some constraints are taken into account (20ms period, temporal coefficients of at least 0.1 ms and no more than 150 temporal coefficients to simulate the design) (Fig. 1.4).<sup>20,24–26</sup> Once the temporal waves were obtained, we used a high-speed dynamic focimeter,<sup>25</sup> provided with a high-speed camera (3823 fps), to measure the optotunable lens response with and without the correction of dynamic effects (Fig. 1.5) and to evaluate the TF SimVis- simulated lens performance.

The SimVis programmed lens is validated when it mimics the real lens design in terms of TF Visual Strehl ratio, where the peaks of the design are not shifted more than 1/8 diopter from the real lens design and an error in the Visual Strehl ratio (height) is less than 10%, 2.5 times the repeatability of the experimental simulations. The number of temporal coefficients will vary according to the real lens design and to the optotunable lens used to simulate the particular design. For the purposes of this study, we simulated three different lenses with the same refractive power (−5.00 D) and

different add powers (low, +1.25 D; medium, +1.75 D; and high, +2.50 D add power MCLs).

## On Bench Through-Focus Optical Quality

Temporal profiles for the different MCL add powers were programmed in the SimVis channel of the AO system. TF optical quality through the SimVis-simulated MCLs was evaluated on bench in the AO visual simulator, using TF double-pass retinal images (DP) and TF retinal images of an E-letter optotype imaged on an artificial eye, following similar procedures as in Vinas et al.<sup>20</sup> For the DP measurements, the artificial eye consisted of a 50.8-mm focal length achromatic doublet lens and a rotating diffuser as an artificial retina. For the IP measurements, the rotating diffuser was replaced with a CCD camera (DCC1240C - High-Sensitivity USB 2.0 CMOS Camera, 1280 × 1024, Global Shutter, Color Sensor; Thorlabs GmbH, Munich, Germany) acting as an artificial “retina.” The stimuli were displayed in the DMD and subtended 1.62°, illuminated with 555-nm light coming from the SCLS. In all measurements, focus shifts were achieved by moving a Badal optometer from +1.00 D to −3.00 D in 0.25-D steps, around the best foci for far.

## In Vivo Measurements on Presbyopic Subjects

TF optical and visual quality were measured in vivo in 10 presbyopic subjects, through SimVis-simulated MCLs and wearing the same real MCLs, by TF DP image series and TF Visual Acuity (VA), respectively. The order of the measurements (MCLs or SimVis) was randomly assigned using a random number generator.

## Subjects

The study was conducted on 10 presbyopic subjects (mean age: 52.3 ± 5.2 years; range: 47 to 64 years; SE: −3.44 ± 0.85 D), habitual CL wearers, who were fit with the corresponding add power MCL, following the manufacturer fit assessment guide.<sup>34</sup> Measurements were performed monocularly, where the eye chosen for the lens fit was the sensorial dominant one. Three subjects were fitted with low (+1.25 D), three subjects with medium (+1.75 D), and four subjects with high (+2.50 D) add power MCLs. All measurements were performed under natural viewing conditions with no dilated eyes. The Table shows the refractive profile and the amount of aberrations (RMS) of the subjects, as well as the refractive base power and add power for

**Table.** Subjects' Refractive and Aberrations Profile

ID	Age (Years)	Pupil Diameter (mm) <sup>a</sup>	Rx (D) <sup>b</sup>	MCL Power (D) <sup>c</sup>	Add (D) <sup>d</sup>	RMS ( $\mu\text{m}$ ) <sup>e</sup>
S#1	51	4.97	-4.75	-5.25	Low	0.48
S#2	48	4.67	-0.50	-0.50	Low	0.31
S#3	47	5.12	-5.50	-5.50	Low	0.86
S#4	48	5.54	-3.25	-3.25	Medium	0.61
S#5	51	3.94	-2.25	-2.50	Medium	0.96
S#6	51	4.18	-1.75	-1.50	Medium	0.14
S#7	51	4.96	-5.00	-5.50	High	0.34
S#8	54	5.37	-3.25	-3.75	High	1.19
S#9	64	4.30	+2.50 -0.75 $\times$ 180	+2.50	High	0.59
S#10	58	4.71	-4.00	-3.75	High	0.97

<sup>a</sup>Natural pupil diameter (mm) obtained from aberrometry.

<sup>b</sup>Autorefractometer refraction.

<sup>c</sup>The base power of the selected MCL.

<sup>d</sup>The add power of the MCL (low: +1.25 D; medium: +1.75 D; high: +2.50 D).

<sup>e</sup>RMS for HOAs, for a 4-mm pupil diameter.

each patient. For baseline information, the RMS for HOAs of the virgin eye (measured with the Hartmann-Shack wavefront sensor) is shown in the last column of the Table.

All participants were acquainted with the nature and possible consequences of the study and provided written informed consent. All protocols met the tenets of the Declaration of Helsinki and had been previously approved by the Spanish National Research Council (CSIC) Bioethical Committee.

### In Vivo Through-Focus Optical and Visual Quality

TF optical quality (DP) and visual quality (VA) measurements were obtained for the subject wearing the real MCL or through the SimVis-simulated MCL. The subjects looked for their best subjective focus while looking at a monochromatic (555 nm) stimulus, starting in positive defocus values relative to their expected best focus. This position (average of five settings by the subject) was taken as the zero. All measurements were performed with a 4-mm artificial pupil.

TF DP retinal aerial images were obtained while the Badal system was moved from +1.00 D to -3.00 D in 0.25-D steps (around the best subjective focus at 555 nm). The subjects foveally fixated the auxiliary spot, while the images were acquired.

TF VA measurements were performed at different positions of the Badal Optometer ranging from +1.00 to -3.00 D in 0.25-D steps. VA was measured using an

8-Alternative Forced Choice (8AFC)<sup>35</sup> procedure with Tumbling E letters and a QUEST (Quick Estimation by Sequential Testing) algorithm programmed with the Psychtoolbox package<sup>36-38</sup> to calculate the sequence of the presented stimulus (letter size and orientation) in the test following the subject's response. The QUEST routine for each VA measurement consisted of 40 trials, each one presented for 0.5 seconds, where the threshold criterion was set to 75%. The VA measurement was estimated as the average of the 10 last stimulus values. The luminance of the stimulus was 20 cd/m<sup>2</sup>. Visual acuity was expressed in terms of logMAR acuity ( $\log\text{MAR} = -\log_{10}[\text{decimal acuity}]$ ).<sup>39</sup> Variability of each VA measurement was obtained from the standard deviation of the 10 last stimulus values used to estimate the threshold in each measurement.

### Data Analysis

The double-pass image quality metric is defined as the maximum intensity of the images,<sup>40</sup> with the intensity values normalized to the no-lens image at best focus. The same analysis was applied to TF DP measurements in subjects. In the case of the E-stimulus, the image quality metric was obtained as the image correlation coefficient (correlation of the image of the E-letter obtained for a given condition with the image of the E-letter with no lens). The conditions (laser power, pupil diameter, exposure time) were kept

constant throughout the entire image series. TF visual quality curves (in subjects) were obtained from TF DP and TF LogMAR VA measurements with the real MCLs and the SimVis-simulated MCLs, as well as the no-lens condition as a reference.

In the case of the TF logMAR VA, depth of focus (DOF) was defined as the range of defocus over which the VA is within the 0.2 logMAR of the subject's best possible acuity, following the procedure by Collins et al.,<sup>41</sup> which corresponds to a visual Strehl of approximately 0.12.<sup>33,42</sup>

The comparison between the real and the SimVis-simulated TF performance was expressed in terms of RMS difference of the linearly interpolated TF curves (in a 4.00 D range), taking the real MCLs as the reference. The RMS difference served as a metric for the goodness of the replication of the lens design by the SimVis simulator.

Statistical analysis was performed with SPSS software (IBM) to test differences across results with the SimVis-simulated and real MCLs (paired-sample *t*-test) in both cases: on-bench and on subjects ( $n = 10$ ). To evaluate the shape similarity of the TF curves, cross correlation of the SimVis-simulated and real MCLs was calculated, and the correlation coefficient ( $\rho$ , similarity, maximum of 1) and lag ( $\kappa$ , offset between the series, minimum of 0) were reported.

## Results

We present TF optical and visual quality of/with MCLs (low, medium and high add powers), for the following conditions: (1) TF optical quality (visual Strehl) of the MCLs alone, calculated from the lens power profiles, which serves as input to the estimation of the SimVis temporal patterns; (2) TF optical quality measurements (double-pass (DP) and one-pass (1P) stimulus images) with the SimVis-simulated MCLs, on bench; (3) TF optical quality (DP) in subjects with the real MCL on eye and with the SimVis-simulated MCL; (4) TF visual quality (VA) in subjects with the real MCL on eye and with the SimVis-simulated MCL.

### Calculated Through-Focus Optical Performance of the Lens Alone

Figure 2 shows the TF Visual Strehl (VS) of the MCL alone calculated from their power profile, for the MCL of low (+1.25 D, blue), medium (+1.75 D, orange) and high (+2.50 D, gray) adds, respectively. The threshold for functional vision ( $VS = 0.12$ )<sup>33,42,43</sup> is marked with a horizontal dashed line. An

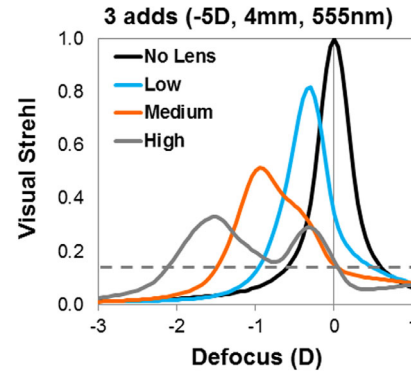


**Figure 2.** TF optical predictions of the lens alone. TF Visual Strehl for the MCL with low (+1.25 D, blue), medium (+1.75 D, orange), and high (+2.50 D, gray) adds, respectively. The no lens condition (black) is shown as a reference. Dashed gray line marks the VS 0.12 threshold for functional vision. Data are for 4-mm pupils.

increase in the near add results in a decrease of maximum VS, a shift of best focus to intermediate vision, and an increase in DOF.

### Through-Focus Optical Performance of the Simvis-Simulated MCLs

Figure 3 shows the TF optical performance of the SimVis-simulated MCLs (low, medium, and high adds) experimentally using a high-speed focimeter. The figure shows data measured with and without correction of the dynamic effects of the optotunable lens. The dynamic correction (to which the green lines correspond in Fig. 3) was implemented for the on-bench and subject measurements. The SimVis-programmed lenses mimic the real lens TF performance (black line) with high accuracy (RMS difference  $< 0.009$ ), with a lateral displacement of the peak less than 1/8 diopter for the three designs.

### Experimental Through-Focus Optical Performance On-Bench

Figure 4 shows TF raw images (upper panel, A) and TF optical quality (lower panels B and C) of the SimVis-simulated MCLs on bench, in the AO system. The top images in each series correspond to DP aerial images. The bottom images in each series correspond to 1P: the E-letter stimulus is captured in a CCD-camera at the "retinal" plane of an artificial eye placed at the position of the subject's eye. The results correspond to low-add lenses (top series in A, blue lines in B/C), medium-add lenses (medium series in A, orange lines in B/C), and high-add lenses (bottom series in A, gray lines in B/C).

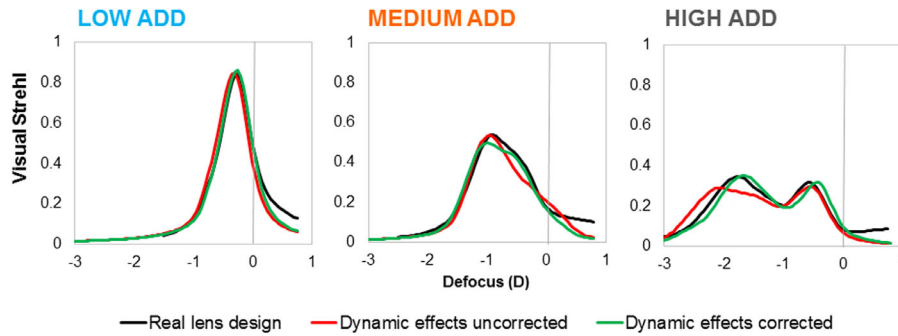


**Figure 3.** TF optical performance of the SimVis-simulated MCLs. TF optical performance of the SimVis-simulated MCLs compared to the real lens design, in terms of TF Visual Strehl ratio, for the low- (left), medium- (center), and high-add (right) powers and for 4-mm pupil diameter. The black line represents the theoretical real lens; the red line represents the SimVis-simulated MCLs when the dynamic effects in the optotunable lens are not corrected; and the green line represents the SimVis-simulated MCLs when the dynamic effects in the optotunable lens are corrected. Data are for 4-mm pupil diameter.

The image quality metric in the DP-images is the maximum intensity in the image (normalized to the intensity of the best focus no-lens image series, Fig. 4B) and in the 1P images an image correlation metric (Fig. 4C), where the 1P image series were correlated to the 0 D-image of the monofocal TF range (4-mm pupil size). The TF data for the no-lens condition (i.e. monofocal, black lines) are shown as a reference. The experimental TF images capture the expected trends of the simulated MCLs: (1) small differences between the low-add lens and no lens condition, as quantified by a shape similarity analysis (DP: lag  $\kappa = 0$ , rho = 0.991; 1P: lag  $\kappa = 0$ , rho = 0.962); (2) Negative shift of the best-focus peak with the medium- and high-add power lenses; (3) broadening of the TF curves for the mid- and high-add lenses.

### Experimental Through-Focus Optical and Visual Quality in Vivo

Figure 5 shows TF double-pass optical quality with the SimVis-simulated MCLs (red lines) and real MCLs (green lines) for all subjects (A) and average data across subjects (C), for all three add powers (low, first column; medium, second column; high, third column). The TF DP optical quality measured with no lens (black dotted lines) is shown as a reference in all cases. Data are shown in similar dioptric range for the real and SimVis-simulated MCLs. TF curves are shifted so that the best subjective focus of the subject matches the center of the TF range (+1.00 D to -3.00 D). TF DP data are expressed in terms of maximum intensity (normalized to the maximum DP aerial image of the no-lens condi-

tion). To compare the different TF curves, the point of maximum intensity of each curve was set as 0D, shifted in some cases from the subjective focus setting by the subject. DP TF curves can only be compared relatively, as the light intensity was adjusted between measurements with and without the MCLs. The blue bars show the difference between real and simulated MCLs curves at each focus position.

The average RMS difference between the real and SimVis-simulated MCLs TF DP curves was  $0.031 \pm 0.003$ ,  $0.025 \pm 0.009$  and  $0.019 \pm 0.009$  for the low-, medium-, and high-adds, respectively. Although there are some cases (S#2, S#7, S#8, and S#10) in which the absolute difference was higher than the mean (RMS =  $0.005 \pm 0.004$ ,  $0.097 \pm 0.002$ ,  $0.062 \pm 0.021$ , and  $0.053 \pm 0.010$ , respectively) the relative shape of the TF curves with the real and the SimVis-simulated lens was very similar (Fig. 5B). The shape similarity metrics for the averaged data were lag  $\kappa = 0$  for all adds, rho = 0.811, rho = 0.792, and rho = 0.861 for the low-, medium-, and high- adds, respectively. Only subjects S#1 and S#7 showed low shape similarity, as shown in Figure 5B. A point-by point comparison of the curves using paired-samples *t*-test resulted in significant differences in subjects S#2 ( $P = 0.003$ ), S#7 ( $P = 0.004$ ), S#8 ( $P < 0.001$ ), and S#10 ( $P < 0.001$ ) (normalized intensity DP test).

Figure 6 shows the TF LogMAR VA with the simulated MCLs (red lines) and real MCLs (green lines) for all subjects (A), and the average data across subjects (C) for all three add powers (low-add, first column; medium-add, second column; high-add, third column). Black dots stand for monofocal VA at the best focus of each subject with no lens. TF curves are shifted so



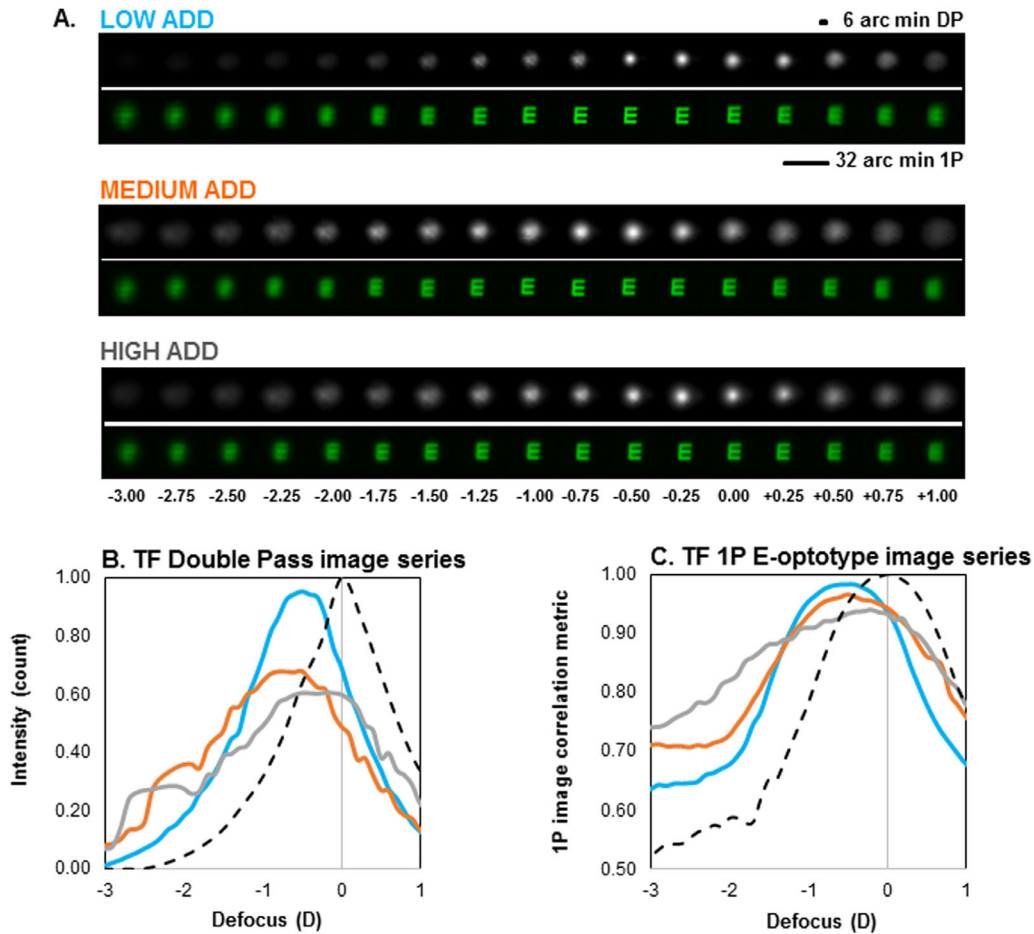


**Figure 4.** TF optical quality on bench and TF optical quality metrics. **(A)** On-bench TF DP aerial retinal images (upper images in each series) of a 250- $\mu\text{m}$  point extended source and TF retinal images (1P) of an E-optotype (bottom images in each series) through the simulated MCLs (series of low-, medium-, and high- adds). *Scale bars* indicate the angular extent of the images (6 arcmin for the DP and 32 arcmin for the 1P images). **(B)** TF DP of image maximum intensity, normalized to the intensity of the best focus no-lens image series; **(C)** TF image correlation metric, each image of the series was correlated to the 0-D image of the monofocal TF range. Blue, Orange and Gray lines correspond to low, medium and high near adds. *Black dotted lines* correspond to a monofocal lens, as a reference.

translational vision science & technology

that the best subjective focus of the subject matches the center of the TF range (+1.00 D to -3.00 D). The blue bars show the difference between real and simulated MCL curves at each focus position. The average RMS difference between the real and SimVis-simulated MCL TF VA curves was  $0.025 \pm 0.008$ ,  $0.015 \pm 0.003$  and  $0.020 \pm 0.011$  for the low, medium and high adds, respectively. A paired *t*-test comparison between TF VA with real and SimVis-simulated MCLs showed statistically significant differences only in the high-add group (low  $P = 0.12$ ; medium  $P = 0.05$ ; high  $P < 0.001$ ), with differences driven by S#7.

The shape similarity metrics between real and SimVis-simulated MCLs for all subjects are shown in Figure 6B, which for average data were  $\text{lag } \kappa = 0$  for all adds,  $\rho = 0.895$ ,  $\rho = 0.944$ , and

$\rho = 0.915$ , for the low-, medium-, and high-adds, respectively, indicating a large degree of similarity. For S#7, showing the largest RMS difference, the shape of the curves showed high similarity ( $\text{lag } \kappa = 0$ ,  $\rho = 0.744$ ). Only S#1 shows low shape similarity. RMS difference for TF DP and for TF VA on subjects showed a significant correlation between results obtained with both methods ( $r = 0.520$ ). Excluding S#7, whose TF DP and TF VA results disagree, there is a significant correlation between shape similarity ( $\rho$ ) for DP and VA (paired-samples *t*-test  $P = 0.047$ ). On average, TF VA was -0.06 at far, 0.13 at intermediate (70 cm), and 0.31 at near (40 cm).

Also, to understand a potential impact of the patient's eye aberrations on the quality of the SimVis-MCL simulation we correlated the Real Lens/SimVis-

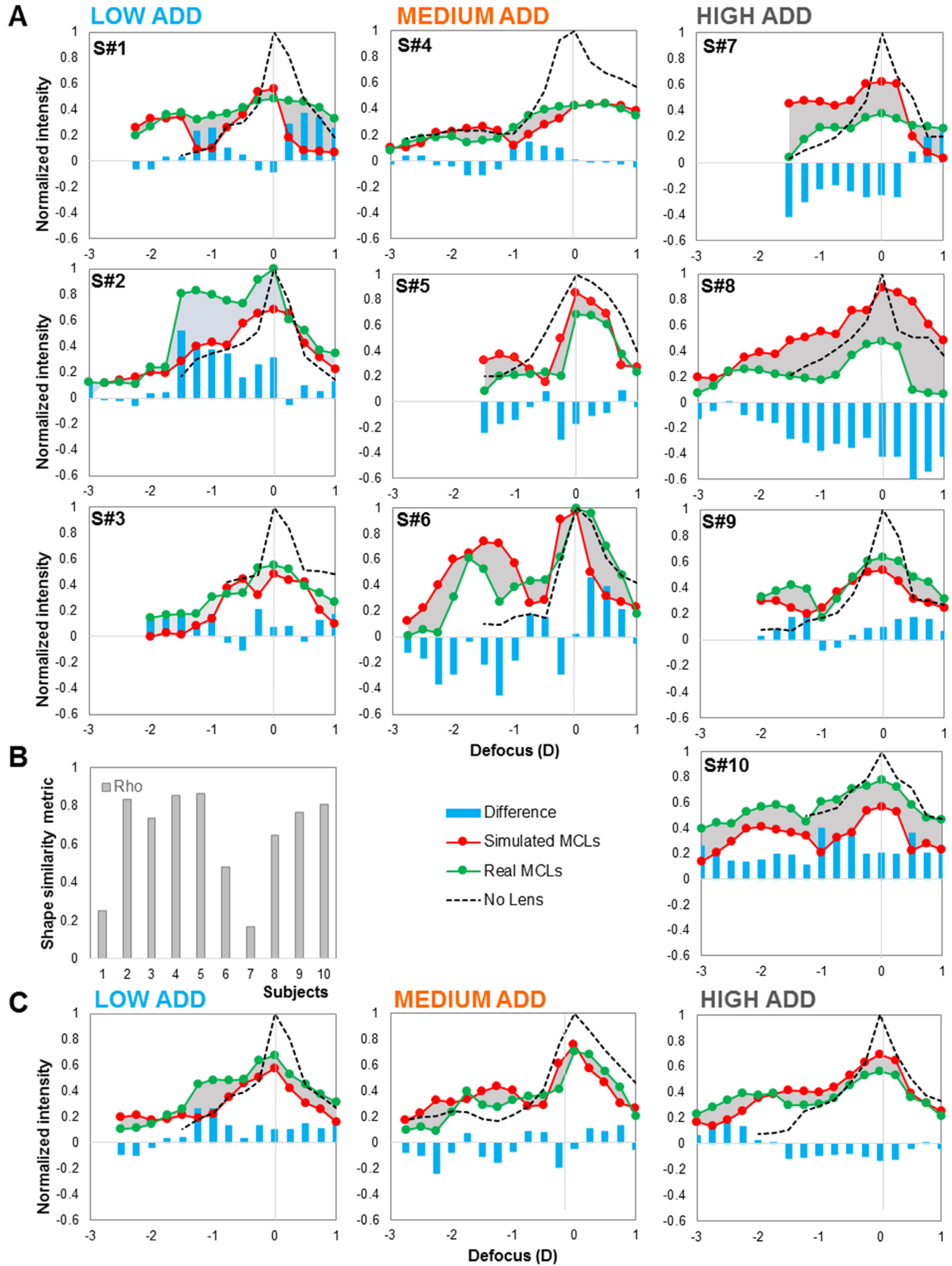


Figure 5. TF DP optical quality. (A) TF DP optical quality (maximum intensity) for all subjects with the simulated MCLs (red lines), the real MCLs (green lines), and no lens (black dotted lines) with all three adds (low-add, first column; medium-add, second column; high-add, third

→

← column). *Blue bars* show the difference between real and simulated MCLs curves. **(B)** Shape similarity metric (crossed correlation,  $\rho$ ) for all subjects. **(C)** Averaged TF DP optical quality with all 3 adds (low-add, first column; medium-add, second column; high-add, third column).

simulated RMS difference (DP & VA) and the RMS wavefront error and found that the goodness of the simulation (RMS difference) was uncorrelated with the optical quality of the virgin eye. Finally, we evaluated potential correlations of these parameters with age and refractive error and did not find significant correlations, although this may be in part associated to the small sample size.

## Discussion

As multifocal contact lenses expand as a solution for presbyopia correction, the understanding of their optical and visual performance, as well as their potential simulation before fitting, becomes important. In this study, we present, to our knowledge, the first combined experimental investigation of the TF performance of multifocal soft contact lenses optically (through double-pass measurements) and visually (through VA).

Several authors<sup>44,45</sup> have reported TF double-pass retinal image quality using a commercial double-pass imaging system (the OQAS, or visual analyzer) by Visiometrics SL (Barcelona, Spain). In general, double-pass systems are better suited than Hartmann-Shack wavefront sensors to characterize optical quality with multifocal contact lenses, particularly for diffractive designs, and zonal refractive designs with relatively abrupt transitions between near and far. Most of the studies on MCLs report TF VA or contrast sensitivity, and a few report aberrometric data with/without the MCLs.<sup>2,46</sup> Only a few studies have used a double-pass technique to study optical quality with MCLs. In 2002, Gispets et al.<sup>47</sup> compared the TF optical quality of two concentric bifocal CLs (center-distance design), using the double-pass technique, and found a better optical quality for distance than for near vision. The authors noted a pupil dependency on the optical performance with those lenses. Also, Pujol et al.<sup>48</sup> evaluated the optical quality at distance, intermediate, and near vision in subjects with and without MCLs and two different pupil sizes (3 and 5 mm) and found that optical quality at near was higher with the MCLs and with 3-mm pupil size and optical quality was lower at distance with the MCLs. More recently, a double-pass technique has been used to measure the TF VA and the objective pseudo accommodation with a soft hydrogel CL for presbyopia (1 day Presbyo, Safilens), finding an

increase in near visual performance and DOF with the presbyopic CL.<sup>49</sup>

We found that although both TF DP and TF VA showed similar trends in the relative performance with the MCLs of different additions, TF DP curves in subjects generally revealed more structure (i.e., peaks and notches) than the TF VA curves. This is likely due to the fact that the DP image intensities (related to Strehl) has a larger contribution from high frequencies (similarly to VS TF curves for the lens alone, Fig. 2) than VA, which may be slightly more insensitive to structured blur, as long as the orientation of the E-letter stimulus is identifiable. These differences can roughly also be observed in the on-bench TF DP and TF 1P (E-letter stimulus), with the latter remaining high over a relatively extensive dioptric range. On the other hand, lack of correspondence between optical and visual quality is not uncommon. Ocular aberrations' wavefront provides an excellent description of the eye's optical quality; however, a direct conversion to VA is not directly interpretable from the wavefront alone. Nankivil et al.<sup>50</sup> showed that, although MTF alone is sufficient to predict population mean VA (in their study, across all measurements, predicted differed from measured [at 4 m] uncorrected VA by +0.01 and best corrected VA by -0.16), it was not sufficient to predict an individual's VA well. Instead, additional factors such as age and spherocylindrical refraction were needed to accurately predict an individual subject's VA, supporting the notion that other factors need to be considered to obtain more accurate estimates of VA.

Several authors have also reported visual performance at various distances with MCLs, specifically with the designs tested in the current study (1-Day-Moist). In a clinical trial on 72 presbyopic eyes, Sha et al.<sup>51</sup> compared high-contrast VA at different vision distances (6 m, 2 m, 1 m, 70 cm, 50 cm, and 40 cm) with three different MCLs (1-Day Acuvue Moist Multifocal [Johnson & Johnson Vision Care]; BioTrue ONEday for Presbyopia [Bausch & Lomb, Rochester, NY, USA]; and Dailies AquaComfort Plus Multifocal [Alcon, Geneva, Switzerland]). They found that BioTrue performed better than Acuvue Moist at distance, AquaComfort Plus performed better than BioTrue at near, and Acuvue Moist performed better than BioTrue and AquaComfort Plus at intermediate and near. In the current study, we found that on average high contrast VA decreased with respect to the best

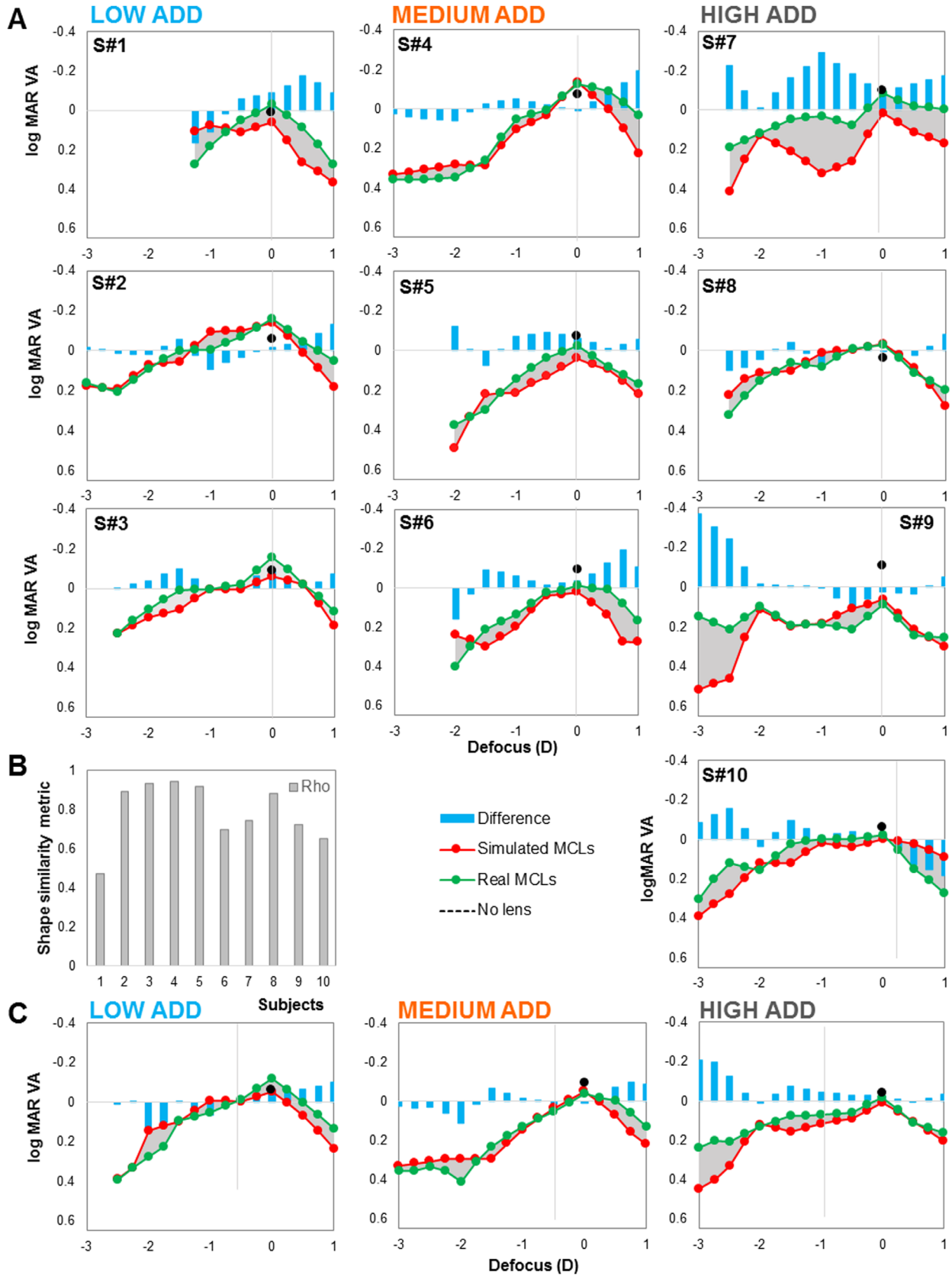


**Figure 6.** TF VA. (A) TF LogMAR VA for all subjects with the simulated MCLs (red lines), and the real MCLs (green lines), with all three adds (low-add, first column; medium-add, second column; high-add, third column). Black dots stand for monofocal VA at the best focus of each subject with no lens. Blue bars show the difference between real and simulated MCL curves. (B) Shape similarity metric (crossed correlation)

→



←  
rho) for all subjects. (C) Averaged TF LogMAR VA with all three adds (low-add, first column; medium-add, second column; high-add, third column).

corrected VA with no-lens, for 4-mm pupil diameters. Our averaged values of logMAR VA at far ( $-0.06$ ), intermediate ( $0.13$ , 70 cm) and near ( $0.31$ , 40 cm), although nominally similar, are generally lower than values from Sha et al.,<sup>51</sup>  $-0.05$ ,  $-0.08$ , and  $0.02$  at those distances (maybe due to the fact that our measurements were performed with a fixed 4-mm, which may be larger than the typical natural pupil diameter at near). Also, our differences in visual acuity across add powers agree with reported values for the same lenses by Moody et al.<sup>52</sup>

We observe a large intersubject variation in the TF performance, even for the same MCL and addition. For example, S#4 and S#5 are subjects of similar age (48 and 51 years old) and MCL base power ( $-3.5$  and  $-2.5$ ) fitted with medium-add MCLs; however, TF DP (Fig. 5) and TF VA (Fig. 6) curves are noticeably broader for S#4 than S#5. The underlying natural optical aberrations (in that particular example, S#4 has better natural optics than S#5) and residual accommodation likely play a role in the intersubject variability, which occurs only in optical measurements (TF DP). Intersubject differences in perception likely play an additional role in the intersubject variability in TF VA.

The difficulty to predict visual performance and visual perception with MCLs make the use of visual simulators clinically relevant. To our knowledge, this is the first study that demonstrates the ability of visual simulators to predict the performance of real commercial multifocal contact lenses in subjects. In particular, we have programmed the 1-Day Moist MCLs in a SimVis system, which operates under the principle of temporal multiplexing. The system had been demonstrated before to simulate refractive and diffractive multifocal IOLs, or theoretical lenses with different energy distributions for near and far.<sup>20</sup> We found a high similarity of the TF optical and visual performance with the MCL on eye and with the SimVis-simulated lens. The average TF performance of the real lens and the simulation was nearly identical, indicating that the SimVis captures to a large extent the lens profile, and that there is no particular bias for the physical MCL to outperform the SimVis-simulated, or viceversa. At the individual level, the salient performance with the SimVis-simulation nominally matches the performance with the real MCL. The differences of the DP retinal intensity metric (real – simulated) are marked only in two subjects. In S#7 and S#1 the DP image intensity

values are much higher (indicative of higher quality) with the SimVis-simulated lens than with the real lens, which may be due to tear film disruption with the contact lens, because the DP metric is very sensitive to scattering. On the other hand, the underestimation of the magnitude of the DP metric with SimVis found in S#5 and S#10 does not have a counterpart in the VA measurements. We did not find that the magnitude of the discrepancy (less than 0.096 RMS difference in all cases) was associated with refractive error, the amount of aberrations or age in this group of subjects. Small variations in design of the 1-Day Moist MCLs for different refractive errors<sup>52</sup> (not programmed in this study) do not seem to have a particular relevance in accounting for the small discrepancies in individual subjects. Other differences between performance of physical contact lenses and the simulations may arise from tear film, contact lens fitting or decentrations (not present in SimVis) and mismatch between pupil size. Also, in previous publications (Akondi et al.<sup>24,33</sup>) we discussed limitations to the fact that SimVis relies on temporal multiplexing to represent a spatial variation in the multifocal lens. While the evaluation in prior work was done for intraocular lenses, several conclusions can be extrapolated to contact lenses, particularly regarding the effect of ocular aberrations and pupil size in refractive lens designs. Also, we demonstrated that smooth varying lens profiles can be simulated using SimVis, provided that the target through-focus optical quality is known, and can be described with a limited number of temporal coefficients (150 temporal coefficients, 5.00 D TF range). Novel MCLs are being designed with surfaces with varying amounts of spherical aberration, also in the transition zones, and their through-focus optical quality can be obtained from the design, using conventional optical design software. The procedure, and the resultant SimVis simulation, has already been validated in intraocular lenses with sophisticated surface geometries (zonal refractive or diffractive).<sup>20</sup> Consequently, novel MCLs could be visually simulated with SimVis, even before they are manufactured.

Our study reveals that the SimVis simulator can be used reliably to provide subjects with the experience of multifocal vision, replicating the visual quality at various distances provided by real contact lenses. The study was performed in an experimental setting, with the Sim+Vis Technology (optotunable lens, operating custom driver and SimVis temporal patterns specif-

ically programmed in this study to replicate those MCLs) implemented in one of the channels of an Adaptive Optics System. Also, the study was performed for fixed pupil diameters (4 mm) and used high contrast visual acuity targets. It is possible to translate the study to the clinical practice with the same SimVis temporal patterns replicating the MCLs programmed in a portable SimVis binocular device (the SimVis Gekko). Future studies will consider natural pupil dynamics (which entails programming the SimVis temporal patterns for a range of pupil diameters) and the use of natural images at far and near to assess visual perception in more realistic conditions.

## Acknowledgments

Supported by the European Research Council (ERC-2011-AdC 294099) to SM; Spanish Government (FIS2017-84753R) to SM, and pre-doctoral fellowship (FPU16/01944) to SA; Collaborative agreement with Johnson & Johnson Vision, Inc., Research & Development, Jacksonville, FL, USA.

Disclosure: **M. Vinas**, 2EyesVision (F); **S. Aissati**, None; **A.M. Gonzalez-Ramos**, None; **M. Romero**, None; **L. Sawides**, 2EyesVision (E, F); **V. Akondi**, 2EyesVision (F); **E. Gambra**, 2EyesVision (E, F); **C. Dorronsoro**, 2EyesVision (E, F); **T. Karkkainen**, Johnson & Johnson Vision (E); **D. Nankivil**, Johnson & Johnson Vision (E); **S. Marcos**, 2EyesVision (F)

## References

1. Richdale K, Mitchell GL, Zadnik K. Comparison of multifocal and monovision soft contact lens corrections in patients with low-astigmatic presbyopia. *Optom Vis Sci* 2006;83:266–273.
2. Charman WN. Developments in the correction of presbyopia I: spectacle and contact lenses. *Ophthalmic Physiol Opt*. 2014;34:8–29.
3. Perez-Prados R, Pinero DP, Perez-Cambrodi RJ, Madrid-Costa D. Soft multifocal simultaneous image contact lenses: a review. *Clin Exp Optom*. 2017;100:107–127.
4. Bennett ES. Contact lens correction of presbyopia. *Clin Exp Optom*. 2008;91:265–278.
5. Madrid-Costa D, Ruiz-Alcocer J, Garcia-Lazaro S, Ferrer-Blasco T, Montes-Mico R. Optical power distribution of refractive and aspheric multifocal contact lenses: Effect of pupil size. *Cont Lens Anterior Eye*. 2015;38:317–321.
6. Kollbaum PS, Bradley A. Correction of presbyopia: old problems with old (and new) solutions. *Clin Exp Optom*. 2020;103:21–30.
7. Lopes-Ferreira D, Fernandes P, Queiros A, Gonzalez-Meijome JM. Combined effect of ocular and multifocal contact lens induced aberrations on visual performance: center-distance versus center-near design. *Eye Contact Lens*. 2018;44(Suppl. 1):S131–S137.
8. Sha J, Bakaraju RC, Tilia D, et al. Short-term visual performance of soft multifocal contact lenses for presbyopia. *Arq Bras Oftalmol*. 2016;79:73–77.
9. Woods J, Woods C, Fonn D. Visual performance of a multifocal contact lens versus monovision in established presbyopes. *Optom Vis Sci*. 2015;92:175–182.
10. Llorente-Guillemot A, Garcia-Lazaro S, Ferrer-Blasco T, Perez-Cambrodi RJ, Cervino A. Visual performance with simultaneous vision multifocal contact lenses. *Clin Exp Optom*. 2012;95:54–59.
11. Gupta N, Naroo SA, Wolffsohn JS. Visual comparison of multifocal contact lens to monovision. *Optom Vis Sci*. 2009;86:E98–105.
12. Plainis S, Ntzilepis G, Atchison DA, Charman WN. Through-focus performance with multifocal contact lenses: effect of binocularity, pupil diameter and inherent ocular aberrations. *Ophthalmic Physiol Opt*. 2013;33:42–50.
13. Bakaraju RC, Ehrmann K, Falk D, Ho A, Papas E. Optical performance of multifocal soft contact lenses via a single-pass method. *Optom Vis Sci*. 2012;89:1107–1118.
14. Lopes-Ferreira D, Fernandes P, Queirós A, González-Meijome JM. Combined effect of ocular and multifocal contact lens induced aberrations on visual performance: center-distance versus center-near design. *Eye Contact Lens*. 2018;44:S131–S137.
15. Vinas M, Dorronsoro C, Radhakrishnan A, et al. Comparison of vision through surface modulated and spatial light modulated multifocal optics. *Biomed Opt Express*. 2017;8:2055–2068.
16. Vinas M, Dorronsoro C, Gonzalez V, Cortes D, Radhakrishnan A, Marcos S. Testing vision with angular and radial multifocal designs using Adaptive Optics. *Vision Res*. 2017;132:85–96.
17. Piers PA, Fernandez EJ, Manzanera S, Norrby S, Artal P. Adaptive optics simulation of intraocular lenses with modified spherical aberration. *Invest Ophthalmol Vis Sci*. 2004;45:4601–4610.
18. Radhakrishnan A, Dorronsoro C, Marcos S. Differences in visual quality with orientation of a rota-

- tionally asymmetric bifocal intraocular lens design. *J Cataract Refract Surg.* 2016;42:1276–1287.
19. Radhakrishnan A, Dorronsoro C, Sawides L, Marcos S. Short-term neural adaptation to simultaneous bifocal images. *Plos One.* 2014;9:e93089.
  20. Vinas M, Benedi-Garcia C, Aissati S, et al. Visual simulators replicate vision with multifocal lenses. *Sci Rep.* 2019;9:1539.
  21. de Gracia P, Dorronsoro C, Sanchez-Gonzalez A, Sawides L, Marcos S. Experimental simulation of simultaneous vision. *Invest Ophthalmol Vis Sci.* 2013;54:415–422.
  22. Dorronsoro C, Radhakrishnan A, de Gracia P, Sawides L, Marcos S. Perceived image quality with simulated segmented bifocal corrections. *Biomed Opt Express.* 2016;7:4388–4399.
  23. Dorronsoro C, Radhakrishnan A, Alonso-Sanz JR, et al. Portable simultaneous vision device to simulate multifocal corrections. *Optica.* 2016;3:918–924.
  24. Akondi V, Dorronsoro C, Gamba E, Marcos S. Temporal multiplexing to simulate multifocal intraocular lenses: theoretical considerations. *Biomed Opt Express.* 2017;8:3410–3425.
  25. Dorronsoro C, Barcala X, Gamba E, et al. Tunable lenses: dynamic characterization and fine-tuned control for high-speed applications. *Optics Express.* 2019;27:2085–2100.
  26. Vinas M, Aissati S, Romero M, et al. Pre-operative simulation of post-operative multifocal vision. *Biomed Opt Express.* 2019;10:5801–5817.
  27. Woodward MA, Randleman JB, Stulting RD. Dissatisfaction after multifocal intraocular lens implantation. *J Cataract Refract Surg.* 2009;35:992–997.
  28. Kim E, Bakaraju RC, Ehrmann K. Power profiles of commercial multifocal soft contact lenses. *Optom Vis Sci.* 2017;94:183–196.
  29. Vinas M, Dorronsoro C, Cortes D, Pascual D, Marcos S. Longitudinal chromatic aberration of the human eye in the visible and near infrared from wavefront sensing, double-pass and psychophysics. *Biomed Opt Exp.* 2015;6:948–962.
  30. Artal P, Marcos S, Navarro R, Williams DR. Odd aberrations and double-pass measurements of retinal image quality. *J Opt Soc Am A Opt Image Sci Vis.* 1995;12:195–201.
  31. Marsack JD, Thibos LN, Applegate RA. Metrics of optical quality derived from wave aberrations predict visual performance. *J Vis.* 2004;4:322–328.
  32. Iskander DR. Computational aspects of the visual Strehl ratio. *Optom Vis Sci.* 2006;83:57–59.
  33. Akondi V, Sawides L, Marrakchi Y, Gamba E, Marcos S, Dorronsoro C. Experimental validations of a tunable-lens-based visual demonstrator of multifocal corrections. *Biomed Opt Express.* 2018;9:6302–6317.
  34. Moody K, Hickson-Curran S, Wooley B, Ruston D. Innovating for multifocal fitting success. *Optician.* 2015;249:6512–6517.
  35. Ehrenstein WH, Ehrenstein A. Psychophysical methods. In: Windhorst U, Johansson H, (eds). *Modern techniques in neuroscience research.* Springer; 1999:1211–1240.
  36. Brainard DH. The Psychophysics Toolbox. *Spatial Vis.* 1997;10:433–436.
  37. Pelli DG. The VideoToolbox software for visual psychophysics: transforming numbers into movies. *Spatial Vis.* 1997;10:437–442.
  38. Kleiner M, Brainard D, Pelli D, Ingling A, Murray R, Broussard C. What's new in psychtoolbox-3. *Perception.* 2007;36:1–16.
  39. Holladay JT. Proper method for calculating average visual acuity. *J Refract Surg.* 1997;13:388–391.
  40. Marcos S, Moreno E, Navarro R. The depth-of-field of the human eye from objective and subjective measurements. *Vis Res.* 1999;39:2039–2049.
  41. Collins MJ, Franklin R, Davis BA. Optical considerations in the contact lens correction of infant aphakia. *Optom Vis Sci.* 2002;79:234–240.
  42. Yi F, Iskander DR, Collins M. Depth of focus and visual acuity with primary and secondary spherical aberration. *Vis Res.* 2011;51:1648–1658.
  43. Cheng X, Bradley A, Thibos LN. Predicting subjective judgment of best focus with objective image quality metrics. *J Vis.* 2004;4:310–321.
  44. Gouvea L, GOt Waring, Brundrett A, Crouse M, Rocha KM. Objective assessment of optical quality in dry eye disease using a double-pass imaging system. *Clin Ophthalmol.* 2019;13:1991–1996.
  45. de Juan V, Aldaba M, Martin R, Vilaseca M, Hererras JM, Pujol J. Optical quality and intraocular scattering assessed with a double-pass system in eyes with contact lens induced corneal swelling. *Cont Lens Anterior Eye.* 2014;37:278–284.
  46. Sivardeen A, Laughton D, Wolffsohn JS. Randomized Crossover Trial of Silicone Hydrogel Presbyopic Contact Lenses. *Optom Vis Sci.* 2016;93:141–149.
  47. Gispets J, Arjona M, Pujol J. Image quality in wearers of a centre distance concentric design bifocal contact lens. *Ophthalmic Physiol Opt.* 2002;22:221–233.
  48. Pujol J, Gispets J, Arjona M. Optical performance in eyes wearing two multifocal contact lens designs. *Ophthalmic Physiol Opt.* 2003;23:347–360.

49. Montani G. Objective and subjective visual performance of a new daily soft contact lens for presbyopia. *Contact Lens Ant Eye*. 2018;41:S25.
50. Nankivil D, Raymond T, Hofmann G, Neal D. Estimating visual acuity from a single wavefront measurement. *SPIE BiOS: SPIE*; 2020;11218:1121822.
51. Sha J, Tilia D, Kho D, et al. Visual performance of daily-disposable multifocal soft contact lenses: a randomized, double-blind clinical trial. *Optom Vis Sci*. 2018;95:1096–1104.
52. Moody K, Karkkainen T, Clark R, Xu J, Hickson-Curran S. Visual acuity performance across different near ADD powers with a new multifocal daily disposable lens. *Contact Lens Ant Eye*. 2018;41(Suppl. 1):s24.